Fermi National Accelerator Laboratory

FERMILAB-Pub-96/139-E
E687

Analysis of the Cabibbo Suppressed Decay D$^0 \rightarrow \pi^- l^+ \nu$

P.L. Frabetti et al.
The E687 Collaboration

Fermi National Accelerator Laboratory
P.O. Box 500, Batavia, Illinois 60510

June 1996

Submitted to *Physics Letters B*

Operated by Universities Research Association Inc. under Contract No. DE-AC02-76CHO3000 with the United States Department of Energy

Analysis of the Cabibbo Suppressed Decay $D^0 \to \pi^- l^+ \nu$

E687 Collaboration

P. L. Frabetti

Dip. di Fisica dell'Università and INFN - Bologna, I-40126 Bologna, Italy

H. W. K. Cheung[a], J. P. Cumalat, C. Dallapiccola[b], J. F. Ginkel, W. E. Johns[c], M. S. Nehring[d]

University of Colorado, Boulder, CO 80309, USA

J. N. Butler, S. Cihangir, I. Gaines, P. H. Garbincius, L. Garren, S. A. Gourlay, D. J. Harding, P. Kasper, A. Kreymer, P. Lebrun, S. Shukla, M. Vittone

Fermilab, Batavia, IL 60510, USA

S. Bianco, F. L. Fabbri, S. Sarwar, A. Zallo

Laboratori Nazionali di Frascati dell'INFN, I-00044 Frascati, Italy

R. Culbertson[e], R. W. Gardner, R. Greene[f], J. Wiss

University of Illinois at Urbana-Champaign, Urbana, IL 61801, USA

G. Alimonti, G. Bellini, M. Boschini, D. Brambilla, B. Caccianiga, L. Cinquini[g], M. Di Corato, M. Giammarchi, P. Inzani, F. Leveraro, S. Malvezzi, D. Menasce, E. Meroni, L. Moroni, D. Pedrini, L. Perasso, F. Prelz, A. Sala, S. Sala, D. Torretta[a]

Dip. di Fisica dell'Università and INFN - Milano, I-20133 Milan, Italy

D. Buchholz, D. Claes[h], B. Gobbi, B. O'Reilly[g]

Northwestern University, Evanston, IL 60208, USA

J. M. Bishop, N. M. Cason, C. J. Kennedy[i], G. N. Kim[j], T. F. Lin, D. L. Puseljic[k], R. C. Ruchti, W. D. Shephard, J. A. Swiatek[l], Z. Y. Wu[m]

University of Notre Dame, Notre Dame, IN 46556, USA

V. Arena, G. Boca, C. Castoldi, G. Gianini, S. P. Ratti, C. Riccardi, L. Viola, P. Vitulo
Dip. di Fisica Nucleare e Teorica dell'Università and INFN - Pavia, I-27100 Pavia, Italy

A. Lopez, University of Puerto Rico at Mayaguez, Puerto Rico

G. P. Grim, V. S. Paolone, P. M. Yager, University of California-Davis, Davis, CA 95616, USA

J. R. Wilson, University of South Carolina, Columbia, SC 29208, USA

P. D. Sheldon, Vanderbilt University, Nashville, TN 37235, USA

F. Davenport, University of North Carolina-Asheville, Asheville, NC 28804, USA

G.R. Blackett, K. Danyo, M. Pisharody, T. Handler
University of Tennessee, Knoxville, TN 37996, USA

B. G. Cheon, J. S. Kang, K. Y. Kim
Korea University, Seoul 136-701, Korea

Results for the Cabibbo suppressed semileptonic decays $D^0 \to \pi^- e^+ \nu$ and $D^0 \to \pi^- \mu^+ \nu$ (charge conjugates are implied) are reported by Fermilab photoproduction experiment E687. We find 45.4 ± 13.3 events in the electron mode and 45.6 ± 11.8 in the muon mode. The relative branching ratio $\frac{BR\ (D^0 \to \pi^- l^+ \nu)}{BR\ (D^0 \to K^- l^+ \nu)}$ for the combined sample is measured to be 0.101 ± 0.020 (stat) ± 0.003 (syst) [1] .

Historically, semileptonic decays have been a productive area in which to study weak decays of hadrons, providing information on the weak currents and the Cabibbo-Kobayashi-Maskawa (CKM) mixing matrix [2]–[6] . With the Cabibbo allowed semileptonic decays well established, experiments have begun turning their attention toward the more elusive Cabibbo suppressed semileptonic charm decays ($D \to \pi\ l\ \nu$ and $D \to \varrho\ l\ \nu$). These decays may be used to compare the functional dependence of form factors between Cabibbo favored and Cabibbo suppressed hadronic currents. In addition, a recent publication[7] has suggested that a thorough understanding of the decay $D^0 \to \pi^- l^+ \nu$ can improve the measurement of V_{ub}. The MARK III[8] and CLEO[9][10] collaborations have provided previous evidence for the decays $D^0 \to \pi^- e^+ \nu$ and $D^+ \to \pi^0 e^+ \nu$. In this paper we report the results of the analysis of the Cabibbo suppressed semileptonic decays $D^0 \to \pi^- e^+ \nu$ and $D^0 \to \pi^- \mu^+ \nu$ relative to the Cabibbo favored modes $D^0 \to K^- e^+ \nu$ and $D^0 \to K^- \mu^+ \nu$, performed on data collected by the photoproduction Experiment E687 at the Fermi National Accelerator Laboratory.

In E687, charm particles were produced by photons with average tagged energy of approximately 200 GeV colliding on a $\sim$ 4 cm long Beryllium target and were detected by a wide-acceptance, multi-purpose spectrometer which is described in detail elsewhere [11]. Charged particle tracks and momentum were measured utilizing a high resolution silicon microstrip detector, five stations of multi-wire proportional chambers, and two large magnets operated with opposite polarities. A system of three multicell Čerenkov detectors working in threshold mode provided charged hadron identification ($\pi^\pm, K^\pm, p^\pm$) over a large momentum range. Two electromagnetic calorimeters, each composed of alternating layers of lead and scintillators, were used to detect electrons in complementary regions of the spectrometer: the inner electromagnetic calorimeter covered the forward region and detected particles passing through the fields of the two magnets; the outer electromagnetic calorimeter covered the outer angular anulus described by particles passing through the field of the first magnet alone. Muons were identified in the forward region of the spectrometer by the inner muon detector, composed of three scintillator arrays and four proportional tube planes; shielding was provided by the upstream detectors (mainly the inner electromagnetic and the hadronic calorimeter) and two blocks of steel.

Approximately $100,000$ charm particles were fully reconstructed from data collected during two approximately equal running periods (the 1990 and the 1991 runs). This analysis is based on a skim of the full data sample which required at least two vertices, each composed of at least two silicon tracks, with a minimum significance of separation.

In order to reduce backgrounds we perform a $D^{*+} - tag$ analysis, i.e. we reconstruct the decay chain $D^{*+} \to D^0\tilde{\pi}^+$, $D^0 \to h^- l^+ \nu$ ($\tilde{\pi}^+$ is the soft pion emitted in the D^{*+} decay, $h^- = \pi^-, K^-$ is the daughter hadron emitted in the D^0 decay and $l^+ = e^+, \mu^+$ is the daughter lepton; charged conjugate states are implicitly assumed throughout this paper). Whenever possible, we use the same requirements for the four decays: $D^0 \to K^-\mu^+\nu$, $D^0 \to \pi^-\mu^+\nu$, $D^0 \to K^-e^+\nu$, and $D^0 \to \pi^-e^+\nu$.

We select two oppositely charged tracks compatible with being a h^-l^+ pair. The h^- hadron must be identified by the Čerenkov counters as kaon consistent in the $D^0 \to K^-l^+\nu$ decay and as pion consistent in the $D^0 \to \pi^-l^+\nu$ decay. Leptons in both decays must not be compatible with being a kaon or a proton in the Čerenkov counters. We require the momentum of both the daughter hadrons (from $D^0 \to K^-e^+\nu$ and $D^0 \to \pi^-e^+\nu$) be greater than 10 GeV/c. Leptons which are identified in either the inner muon system or the inner electromagnetic calorimeter must also have momentum greater than 10 GeV/c and electrons identified by the outer electromagnetic calorimeter must have momentum greater than 6 GeV/c. The two daughter tracks are required to originate from a common vertex in space (D^0 decay vertex or secondary vertex) with a confidence level greater than 1%. We compute the invariant mass of the h^-l^+ pair, and we restrict it to the range 0.95 $GeV/c^2 < M(K^-l^+) < 1.85$ GeV/c^2 and 1.1 $GeV/c^2 < M(\pi^-l^+) < 1.85$ GeV/c^2. This cut reduces contamination from other incompletely reconstructed D^0 tag semileptonic decays (such as $D^0 \to K^{*-}l^+\nu$ and $D^0 \to \varrho^-l^+\nu$) for which the hadron–lepton invariant mass distribution is shifted to lower values.

The primary vertex of the event is reconstructed by an algorithm which uses all the microvertex tracks in the event (except the two tracks already assigned to the secondary vertex) to form all possible vertices with a confidence level greater than 1%. We choose the primary vertex to be the highest multiplicity vertex reconstructed within the target limits, which has a significance of separation from the secondary vertex of $\ell/\sigma > 4$ [12] . To further reduce background from higher charged multiplicity semileptonic decays, we consider all other tracks in the event (i.e the tracks not already used for the primary or secondary vertices), and we require the confidence level that any of these tracks form a vertex with the two decay prongs, h^-, l^+, to be less than 1%. Due to heavy combinatoric background in the outer region of the spectrometer, decays which are reconstructed using the outer electromagnetic calorimeter are subject to an additional vertexing cut. Namely, we require the confidence level that either the daughter hadron or lepton are consistent with originating from the primary vertex to be less than 10%.

The primary and secondary vertex positions define a direction of flight for the candidate D^0, and the D^0 momentum is computed by assuming the D^0 mass. Following the technique developed by E691 [13], we perform the calculation in a boosted frame where the total charged momentum (i.e. the momentum of the $h^- l^+$ pair) is perpendicular to the D^0 direction of flight. In performing the calculation, we impose physical constraints on the energy and momentum of the neutrino in the boost frame: $E'(\nu) \geq 0\ GeV/c^2$ and $P_L'^2(\nu) > -2\ GeV/c^2$. Slightly negative values of $P_L'^2(\nu)$ are allowed because of resolution effects, but for these events we set $P_L'^2(\nu) = 0\ GeV/c^2$ in the computation which follows. We obtain the D^0 momentum in the boost frame with a *twofold ambiguity*: $P'(D^0) = \pm\sqrt{P_L'^2(\nu)}$. The ambiguity persists when the D^0 momentum is boosted back to the laboratory frame, resulting in two D^0 momentum solutions (the two solutions coincide if $P_L'(\nu) = 0$).

We combine the D^0 momentum with the momentum of the soft pion $\tilde{\pi}^+$ to compute the D^{*+} invariant mass. The $\tilde{\pi}^+$ candidate must be assigned to the primary vertex, it must have the same charge as the daughter lepton, and its Čerenkov identification must be pion consistent. The twofold ambiguity is arbitrated by choosing the lowest D^{*+} mass solution: Monte Carlo studies show that this choice is correct approximately 80% of the time given our acceptance.

In Figures 1 (a)-(c) and 2 (a)-(c) we show (as solid points) the $D^{*+} - D^0$ mass difference for $D^0 \rightarrow K^- l^+ \nu$ and $D^0 \rightarrow \pi^- l^+ \nu$ candidates, where the lepton (l^+) is either a muon or an electron[14]. In order to measure the amount of signal present in the plots, it is necessary to understand the sources of background which may contaminate the invariant mass distributions. We do not use *wrong-sign* (WS) histograms to parametrize the background in the *right-sign* (RS) histograms[15]. Although random combinatoric background is expected to affect RS and WS in the same way, background from other charm decays can preferentially affect one or the other [16]. Rather, for each possible source of background we try to quantitatively estimate the amount of contamination in the data histograms based on our knowledge of decay branching ratios, Monte Carlo efficiencies, Monte Carlo signal shapes, and misidentification probabilities.

The fit of the data histograms is performed with a *binned maximum likelihood* technique. For each histogram, the likelihood is defined as:

$$\mathcal{L} = \prod_{i=1}^{\#bins} \frac{n_i^{s_i} e^{-n_i}}{s_i!} \ ,$$

where:

s_i = number of events in bin i of data histogram,

n_i = number of events in bin i of fit histogram .

The fit histogram is constructed using the shape of the $D^0 \to h^- l^+ \nu$ signal from Monte Carlo and the estimated amount of contamination from all relevant sources of background.

For the $D^0 \to K^- l^+ \nu$ case, the fit histogram is constructed as:

$$n_i = Y_{Kl\nu}\ S_{1i} + Y_{2,K^*l\nu}\ S_{2i} + \mathcal{M}\ S_{3i} + \mathcal{X}\ S_{4i}\ ,$$

where $Y_{Kl\nu}$ is the fitted yield for the $D^0 \to K^- l^+ \nu$ signal; $Y_{2,K^*l\nu}$ represents the amount of contamination from the decay $D^{*+} \to D^0 \tilde{\pi}^+$, $D^0 \to K^{*-} l^+ \nu$, $K^{*-} \to K^- \pi^0$ (where the π^0 is not reconstructed); $\mathcal{M}$ is the estimated amount of contamination from decays where hadrons are misidentified as leptons (for example, $D^0 \to K^- \pi^+ \pi^0$ or $D^0 \to K^- \pi^+ \pi^0 \pi^0$, where the π^+ is misidentified as a lepton l^+ and the π^0 is not reconstructed); $\mathcal{X}$ represents the amount of random combinatoric background, and the S_{ji}'s are the normalized shapes of the different fit components ($\sum_{i=1}^{\#bins} S_i = 1$). The level of $K^{*-} l^+ \nu$ contamination is estimated as $Y_{2,K^*l\nu} = Y_{Kl\nu}\ \frac{BR\ (D^0 \to K^{*-} l^+ \nu)\ BR\ (K^{*-} \to K^- \pi^0)}{BR\ (D^0 \to K^- l^+ \nu)}\ \frac{\epsilon(K^* l\nu, K^* \to K^- \pi^0)}{\epsilon(Kl\nu)}$ (ϵ denotes a reconstruction efficiency and BR a branching ratio). To measure the amount of hadron/lepton misidentification background, we run our analysis algorithm on a subsample (about $\sim 10\%$) of our total data sample *without* the lepton identification requirement, and weight each entry in the corresponding $D^{*+} - D^0$ mass difference plot according to the momentum-dependent probability of misidentifying a hadron as a lepton. We then boost the amount of background by the ratio of charm yield in the total data sample relative to the charm yield in the subsample considered (the $D^0 \to K^- \pi^+$ yield was used as the charm estimator). The level and shape of misidentified background are entered as a *fixed* component in the fit histogram. Finally, we estimate the shape of the random combinatoric background [17] using both data and Monte Carlo and enter it with a *variable* amplitude in the fit histogram.

For the $D^0 \to \pi^- l^+ \nu$ case, the fit histogram is constructed as:

$$n_i = Y_{\pi l\nu}\ S_{5i} + Y'_{Kl\nu}\ S_{6i} + Y_{7,K^*l\nu}\ S_{7i} + Y_{8,K^*l\nu}\ S_{8i} + Y_{\varrho l\nu}\ S_{9i} + \mathcal{M}\ '\ S_{10i} + \ \mathcal{X}\ '\ S_{11i}\ ,$$

where $Y_{\pi l\nu}$ is the fitted yield for the $D^0 \to \pi^- l^+ \nu$ signal; $Y'_{Kl\nu} = Y_{Kl\nu}\ \frac{\epsilon(Kl\nu\ as\ \pi l\nu)}{\epsilon(Kl\nu)}$ is the amount of feedthrough from the $D^0 \to K^- l^+ \nu$ signal to the $D^0 \to \pi^- l^+ \nu$ histogram due to K/π misidentification; $Y_{7,K^*l\nu}$ and $Y_{8,K^*l\nu}$ are the amounts of contamination from the $D^{*+} - tag$ decays $D^0 \to K^{*-} l^+ \nu$, $K^{*-} \to K^- \pi^0$ (K^- misidentified as π^-) and $D^0 \to K^{*-} l^+ \nu$, $K^{*-} \to \overline{K^0} \pi^-$ ($\overline{K^0}$ not reconstructed) and are estimated as before; $Y_{\varrho l\nu}$ is the background from the decay

$D^0 \to \varrho^- l^+ \nu$; $\mathcal{M}\ '$ is the estimated background from hadron/lepton misidentification (fixed in the fit); and finally $\mathcal{X}\ '$ is the amount of random combinatoric background (which varies in the fit). Background from the decay $D^0 \to \varrho^- l^+ \nu$ will contribute to the $D^0 \to \pi^- l^+ \nu$ signal at a level which depends on the branching ratio $\frac{BR\ (D^0 \to \varrho^- l^+ \nu)}{BR\ (D^0 \to \pi^- l^+ \nu)}$. Since this decay has not been observed, we estimate the amount of contamination by using the measured value for the branching ratio $\frac{BR\ (D^+ \to \varrho^0 l^+ \nu)}{BR\ (D^+ \to K^{*0} l^+ \nu)} = 0.044^{+0.031}_{-0.025} \pm 0.014$ [18] and assuming $\frac{B(D^0 \to \varrho^- l^+ \nu)}{B(D^0 \to K^{*-} l^+ \nu)} \equiv 2 \times \frac{B(D^+ \to \varrho^0 l^+ \nu)}{B(D^+ \to K^{*0} l^+ \nu)}$ (from isospin). The number of $D^0 \to \varrho^- l^+ \nu$ events which enter the $D^0 \to \pi^- l^+ \nu$ signal is estimated as: $Y_{\varrho l \nu} = \frac{Y(K^- l^+ \nu)}{\epsilon(K^- l^+ \nu)} \times \frac{BR(D^0 \to K^{*-} l^+ \nu)}{BR(D^0 \to K^- l^+ \nu)} \times \frac{BR(D^0 \to \varrho^- l^+ \nu)}{BR(D^0 \to K^{*-} l^+ \nu)} \times \epsilon(\varrho l \nu \text{ as } \pi l \nu)$, where $\epsilon(\varrho l \nu \text{ as } \pi l \nu)$ is the efficiency for reconstructing the decay $D^0 \to \varrho^- l^+ \nu$ as $D^0 \to \pi^- l^+ \nu$.

We perform separate fits for the muon sample, the electron sample detected in the inner electromagnetic calorimeter, and the electron sample detected in the outer calorimeter; also, we fit separately for the 1990 and 1991 runs. For each of these six subsamples, we maximize the following quantity:

$$\mathcal{L} = \mathcal{L}_{Kl\nu} \times \mathcal{L}_{\pi l \nu} \times exp\left\{ -\frac{1}{2} \left[\frac{\mathcal{A} - A_0}{\sigma_{A_0}} \right]^2 \right\} \times exp\left\{ -\frac{1}{2} \left[\frac{\mathcal{B} - B_0}{\sigma_{B_0}} \right]^2 \right\} ,$$

where $\mathcal{L}_{Kl\nu}$, $\mathcal{L}_{\pi l \nu}$ are the likelihood functions for the $K^- l^+ \nu$ and $\pi^- l^+ \nu$ histograms, respectively. The two Gaussian terms have been added to the likelihood to allow the branching ratios $\mathcal{A} = \frac{BR\ (D^0 \to K^{*-} l^+ \nu)}{BR\ (D^0 \to K^- l^+ \nu)}$, $\mathcal{B} = \frac{BR(D^0 \to \varrho^- l^+ \nu)}{BR(D^0 \to K^{*-} l^+ \nu)}$ to fluctuate within their error around their measured values $A_0 = 0.60 \pm 0.06$ [19] [20] [21] and $B_0 = 0.088 \pm 0.056$ [18], respectively. The combined likelihood $\mathcal{L}$ depends on six parameters: $Y_{Kl\nu}$, $Y_{\pi l \nu}$, $\mathcal{X}$, $\mathcal{X}\ '$, $\mathcal{A}$ and $\mathcal{B}$; therefore we fit *simultaneously* for the $K^- l^+ \nu$ and $\pi^- l^+ \nu$ yields. For each subsample, we use the fitted yields to compute the branching ratio:

$$\frac{BR\ (D^0 \to \pi^- l^+ \nu)}{BR\ (D^0 \to K^- l^+ \nu)} = \frac{Y_{\pi l \nu}/\epsilon(\pi l \nu)}{Y_{Kl\nu}/\epsilon(Kl\nu)} \ .$$

In Figures 1 (a)-(f) and 2 (a)-(f) we show (as solid lines) the final fits to the $D^0 \to K^- l^+ \nu$ and $D^0 \to \pi^- l^+ \nu$ data histograms, together with the various fit components (different hatching styles). The fitted yields for the various components are listed in Table I. In Table II we report the relative branching ratio measurements for the independent muon and electron subsamples. For each subsample, the quoted statistical error includes the correlation term between $Y_{\pi l \nu}$ and $Y_{Kl\nu}$, the errors due to the finite size of our generated Monte Carlo samples, and the statistical errors in the two branching ratios A_0 and B_0 which are used in the fit.

Extensive studies were performed to determine the systematic error on our measurement. We found that the major sources of systematics come from Čerenkov particle identification, uncertainty in the fraction of hadrons misidentified as leptons and possible variations of the fitting process. We found no evidence for systematic errors due to lepton identification, which is in large part due to the nearly identical event topologies of $D^0 \to K^- l^+ \nu$ and $D^0 \to \pi^- l^+ \nu$. Any systematic variation between data and Monte Carlo in lepton identification should effectively cancel when the ratio of the modes is taken. To estimate errors incurred through the use of various analysis cuts, the data were divided into four approximately equal, statistically independent subsamples in several variables including ℓ/σ , the confidence level of the secondary vertex, lepton momentum, daughter–hadron momentum, and hadron–lepton invariant mass. We found no evidence for systematic errors in any of these variables. Errors associated with our chosen fitting technique were estimated by considering reasonable variations of the fitting process. The mass range over which the fit is performed, the bin size, and the shape of the random background component of our fits were all varied. The results of all these fits were then statistically combined to obtain the "fit variants" systematic error. Finally, all the individual sources of systematic error were combined in quadrature to compute the total systematic error.

We found that a large source of uncertainty to the branching ratio measurement originates from the parametrization of the form factors entering the hadronic current. When generating the Monte Carlo samples for $D^0 \to K^- l^+ \nu$ and $D^0 \to \pi^- l^+ \nu$ we assumed a single pole mass dependence for the form factors, as it is commonly done in literature[22]:

$$f^h_{\pm}(q^2) = \frac{f^h_{\pm}(0)}{1 - q^2/(M^h_{pole})^2} \ ,$$

where the value of the pole mass has been set to $M^K_{pole} = 2.11\ GeV/c^2$ for the $D^0 \to K^- l^+ \nu$ decay, and to $M^\pi_{pole} = 2.01\ GeV/c^2$ for the $D^0 \to \pi^- l^+ \nu$ decay[23]. We found that the choice of the actual pole mass value significantly affects the hadron–lepton mass distribution (and consequently, the mass cut efficiency) for the $D^0 \to \pi^- l^+ \nu$ decay, while having a negligible effect in the $D^0 \to K^- l^+ \nu$ case (see Figure 3 (a)). In Figure 3 (b) we show how the measured branching ratio changes within a reasonable range of M^π_{pole}[23] (assuming $M^K_{pole} = 2.11\ GeV/c^2$). We do *not* include this source of theoretical uncertainty in the total systematic error.

To combine the branching ratio measurements for the electron and muon modes it is necessary to account for differences in the available phase space due to the larger muon mass. We calculate this correction factor by integrating the full expression for the semileptonic decay rate, including terms proportional to the lepton mass. With our choice of pole masses, and by further assuming $\xi \equiv \frac{f_{-}(0)}{f_{+}(0)} = -1$ [25], we compute a boost factor of 1.01 for the muon mode. Combining the measurements as a weighted average we obtain:

$$\frac{BR\ (D^0 \to \pi^- l^+ \nu)}{BR\ (D^0 \to K^- l^+ \nu)} = 0.101 \pm 0.020 \pm 0.003\ .$$

Assuming as independent variables the hadron-lepton invariant mass squared (m^2_{hl}) and the four momentum transfer squared ($q^2 = m^2_{l\nu}$), the differential decay rate for a pseudoscalar semileptonic decay is written as[26]:

$$\frac{d^2\Gamma\ (D \to hl\nu)}{dq^2 dm^2_{hl}} \propto |V_{cq}|^2\ |f_+^h(q^2)|^2 \left\{ A + B\ Re\ \xi + C\ |\xi|^2 \right\}\ ,$$

where A, B, and C are kinematic factors which depend on m^2_{hl},q^2, and the lepton mass squared (m^2_l). This expression can be used to compute the ratio of the form factors for $D^0 \to \pi^- l^+ \nu$ and $D^0 \to K^- l^+ \nu$ at zero momentum transfer $q = 0$. Using our choice for the parameters M^K_{pole}, M^π_{pole} and ξ, we integrate the differential decay rate over the region of the Dalitz plot (q^2 vs m^2_{hl}) which is defined by the hadron-lepton mass cut used in the analysis. Taking the ratio of the two decays, we obtain:

$$\frac{Y_{\pi l\nu}}{Y_{K l\nu}} = \left|\frac{V_{cd}}{V_{cs}}\right|^2 \left|\frac{f_+^\pi(0)}{f_+^K(0)}\right|^2$$
$$\times \frac{\int_{(1.1)^2}^{(1.85)^2} dm^2_{\pi l} \int_{q^2_{min}}^{q^2_{max}} dq^2 \left|\frac{f_+^\pi(q^2)}{f_+^\pi(0)}\right|^2 \left[A + BRe\xi + C|\xi|^2\right]_{\pi l\nu} \epsilon_{\pi l\nu}(q^2)}{\int_{(0.95)^2}^{(1.85)^2} dm^2_{Kl} \int_{q^2_{min}}^{q^2_{max}} dq^2 \left|\frac{f_+^K(q^2)}{f_+^K(0)}\right|^2 \left[A + BRe\xi + C|\xi|^2\right]_{Kl\nu} \epsilon_{Kl\nu}(q^2)}$$

where the two limits in the inner integration q^2_{min}, q^2_{max} are functions of m^2_{hl}. Here $\epsilon_{hl\nu}(q^2)$ is the reconstruction efficiency for the decay $D^0 \to h^- l^+ \nu$ measured in bins of q^2 and is independent of the specific functional form used for the form factors. In the above equation, only the form factors themselves depend upon the pole masses (or the chosen form factor model). Since there are no experimental measurements for the pole mass in the decay $D^0 \to \pi^- l^+ \nu$, we choose to quote our measurement of the quantity $\left|\frac{V_{cd}}{V_{cs}}\right|^2 \left|\frac{f_+^\pi(0)}{f_+^K(0)}\right|^2$ at the expected pole masses $M^K_{pole} = 2.11\ GeV/c^2$ and $M^\pi_{pole} = 2.01\ GeV/c^2$. The ratio of integrals on the right hand side of the equation can be computed numerically, and by equating it to the ratio of the yields returned by the fit, we determine:

$$\left|\frac{V_{cd}}{V_{cs}}\right|^2 \left|\frac{f_+^\pi(0)}{f_+^K(0)}\right|^2 = 0.050 \pm 0.011 \pm 0.002\ .$$

where, assuming form factor universality, we have combined the individual electron and muon mode measurements (see Table II) into a weighted average. With this technique we take advantage of the fact that the pion-lepton invariant mass cut restricts the accessible range of q^2 in the decay $D^0 \to \pi^- l^+ \nu_l$ to a region well below the maximum value $q^2_{max} = (M_D - M_\pi)^2$ where the different form factor models diverge strongly. In the Cabibbo favored mode the maximum value of q^2 is much lower ($1.88\ GeV^2/c^4$) and consequently the analysis is less sensitive to M^K_{pole} (see Figure 3(a)). In Figure 4 (a) we show how our measurement changes as a function of the $D^0 \to \pi^- l^+ \nu$ pole mass.

The statistical errors on the ratio of form factors are obtained by propagating the errors on the two fitted yields, their correlation term, and the errors on the q^2 binned efficiencies used in the integration. The systematic errors are computed by combining the systematic errors already discussed for the branching ratio measurement with a small contribution originating from different fit techniques for the q^2 binned efficiencies. We performed the study for two different values of the $D^0 \to K^- l^+ \nu$ pole mass [23]. We also checked how sensitive our measurement is to the value of the parameter ξ used in the integration. We considered the measurement $\xi = -1.3^{+3.6}_{-3.4} \pm 0.6$[24] and performed again the integration by varying ξ within $\pm 1\ \sigma$ of its measured value. We found that $\left|\frac{V_{cd}}{V_{cs}}\right|^2 \left|\frac{f^\pi_+(0)}{f^K_+(0)}\right|^2$ changes by $\sim \pm 1.5\%$ when muon data are used.

As an attempt to generalize this result beyond the single pole form factor parameterization, we used the same technique to measure $\left|\frac{V_{cd}}{V_{cs}}\right|^2 \left|\frac{f^\pi_+(0)}{f^K_+(0)}\right|^2$ with linear form factors $f_+(q^2) = (1+aq^2)$ where $0 < a < 0.9$. We present this measurement in Figure 4 (b) as a function of the slope of the pion form factor. If the simple pole form factors are expanded into a series and truncated after the first term, pole masses of 1.9, 2.01, and 2.11 correspond to slopes of 0.277, 0.248, and 0.225 respectively.

Finally, unitarity constraints on the CKM matrix set a value for the ratio $\left|\frac{V_{cd}}{V_{cs}}\right|^2$ at 0.051 ± 0.001[27]; using this value, we can compute the ratio of the form factor normalizations alone to be:

$$\frac{\left|f^\pi_+(0)\right|}{\left|f^K_+(0)\right|} = 1.00 \pm 0.11 \pm 0.02 \ .$$

In Table II we compare our measurements with other experiments and various theoretical models. Our measurement of the relative branching ratio $\frac{BR\ (D^0 \to \pi^- l^+ \nu)}{BR\ (D^0 \to K^- l^+ \nu)}$ is the most accurate to date and is consistent with both previous experimental measurements and a wide range of theoretical calculations. We have observed the decay in both the semi–electronic and semi–muonic channels and the internal agreement between these two samples is excellent. In the future, a more precise measurement of the branching ratio $\frac{BR\ (D^0 \to \pi^- l^+ \nu)}{BR\ (D^0 \to K^- l^+ \nu)}$ and the ratio $\left|\frac{V_{cd}}{V_{cs}}\right|^2 \left|\frac{f^\pi_+(0)}{f^K_+(0)}\right|^2$ will have to come not only from improved statistics, but also from a better experimental measurement of the $D^0 \to \varrho^- l^+ \nu$ contamination to the $D^0 \to \pi^- l^+ \nu$ signal, and an improved theoretical knowledge of the form factors involved in the decay.

We wish to acknowledge the assistance of the staffs of the Fermi National Accelerator Laboratory, the INFN of Italy, and the physics departments of the collaborating institutions. This research was supported in part by the National Science Foundation, the U.S. Department of Energy, the Italian Istituto Nazionale di Fisica Nucleare and Ministero dell'Università e della Ricerca Scientifica e Tecnologica, and the Korean Science and Engineering Foundation.

TABLE I. Yields of different fit components[28]

Decay	μ sample	e sample	Total
$K^- l^+ \nu$	824.5 ± 33.0	681.9 ± 32.5	1506.4 ± 46.3
$(K^- \pi^0)\ l^+ \nu$	79.6 ± 6.6	53.3 ± 3.7	132.9 ± 7.6
$\pi^- l^+ \nu$	45.6 ± 11.8	45.4 ± 13.3	91.0 ± 17.8
$K^- l^+ \nu$, K^- misid as π^-	26.6 ± 1.9	24.5 ± 1.8	51.1 ± 2.6
$(\overline{K^0} \pi^-)\ l^+ \nu$	8.2 ± 0.8	6.1 ± 0.6	14.3 ± 1.0
$(K^- \pi^0)\ l^+ \nu$, K^- misid as π^-	0.5 ± 0.1	0.5 ± 0.1	1.0 ± 0.1
$\varrho^- l^+ \nu$	5.2 ± 2.4	4.2 ± 1.4	9.4 ± 2.8

TABLE II. Measured Quantities

Reference	$\frac{BR\ (D^0 \to \pi^- l^+ \nu)}{BR\ (D^0 \to K^- l^+ \nu)}$
This Work (e)	0.103 ± 0.031 (stat) ± 0.004 (syst)
This Work (μ)	0.099 ± 0.026 (stat) ± 0.007 (syst)
This Work ($e+\mu$)[1]	0.101 ± 0.020 (stat) ± 0.003 (syst)
CLEO[9]	0.103 ± 0.039 (stat) ± 0.013 (syst)
MARK III[8]	$0.11^{+0.07}_{-0.04}$ (stat) ± 0.02 (syst)
CLEO[10][30]	$0.170 \pm 0.054 \pm 0.028$
Scora *et al.*[6]	0.0476 [29]
Lubicz *et al.*[31]	0.086 ± 0.041
Narison[32]	0.083
Demchuk *et al.*[33]	0.073

	$\left\lvert\frac{V_{cd}}{V_{cs}}\right\rvert^2 \left\lvert\frac{f_+^\pi(0)}{f_+^K(0)}\right\rvert^2$	$\left\lvert\frac{f_+^\pi(0)}{f_+^K(0)}\right\rvert$
This Work (e)	$0.054 \pm 0.017 \pm 0.002$	$1.03 \pm 0.16 \pm 0.02$
This Work (μ)	$0.048 \pm 0.014 \pm 0.003$	$0.97 \pm 0.14 \pm 0.03$
This Work ($e+\mu$)	$0.050 \pm 0.011 \pm 0.002$	$1.00 \pm 0.11 \pm 0.02$
CLEO[9]	$0.052 \pm 0.020 \pm 0.007$	$1.01 \pm 0.20 \pm 0.07$
CLEO[10]	$0.085 \pm 0.027 \pm 0.014$	$1.29 \pm 0.21 \pm 0.11$
Lubicz *et al.*[31]		0.92 ± 0.18
Narison[32]		0.91 ± 0.01
Demchuk *et al.*[33]		0.87

REFERENCES

[a] Present address: Fermilab, Batavia, IL 60510, USA.

[b] Present address: University of Maryland, College Park, MD 20742, USA.

[c] Present address: University of South Carolina, Columbia, SC 29208, USA.

[d] Present address: Vanderbilt University, Nashville, TN 37235, USA.

[e] Present address: Enrico Fermi Institute, University of Chicago, Chicago, IL 60637, USA.

[f] Present address: Syracuse University, Syracuse, NY 13244-1130, USA.

[g] Present address: University of Colorado, Boulder, CO 80309, USA.

[h] Present address: University of New York, Stony Brook, NY 11794, USA.

[i] Present address: Yale University, New Haven, CN 06511, USA.

[j] Present address: Pohang Accelerator Laboratory, Pohang, Korea.

[k] Present address: Lawrence Berkeley Laboratory, University of California, Berkeley, CA 94720, USA.

[l] Present address: Science Applications International Corporation, McLean, VA 22102, USA.

[m] Present address: Gamma Products Inc., Palos Hills, IL 60465, USA.

[1] We use a notation where combined results for the electron and muon modes are reported with a generic lepton symbol l. Since in the averaging process the muon branching ratio is scaled by a factor of 1.01 (see text for details), the combined result for the branching ratio is *effectively* normalized to the electron mode.

[2] F.J. Gilman and R.L. Singleton, Phys. Rev. D41, 142 (1990).

[3] W.J. Marciano and A. Sirlin, Phys. Rev. Lett. 56, 22 (1986).

[4] W. Jaus and G. Rasche, Phys. Rev. D35, 3420 (1987).

[5] H. Leutwyler and M. Roos, Z. Phys. C25, 91 (1984).

[6] D. Scora and N. Isgur, Phys. Rev. D52, 2783 (1995).

[7] G. Burdman and J. Kambor, FERMILAB-PUB-96-003-T, Feb 1996.

[8] MarkIII Collab., J. Adler *et al.*, Phys. Rev. Lett. 62, 1821 (1989).

[9] CLEO Collab., F. Butler *et al.*, Phys. Rev. D52, 2656 (1995).

[10] CLEO Collab., M.S, Alam *et al.*, Phys. Rev. Lett. 71, 1311 (1993).

[11] E687 Collab., P. L. Frabetti *et al.*, Nucl. Instrum. Methods. A320, 519 (1992).

[12] ℓ is the distance in space between the reconstructed primary and secondary vertices, and σ_ℓ is the corresponding error computed on an event by event basis.

[13] E691 Collab., J.C. Anjos *et al.*, Phys. Rev. Lett. 62, 1587 (1989).

[14] We prefer to plot the $D^{*+} - D^0$ mass difference instead of the D^{*+} mass, even if the D^0 mass is fixed to its nominal value.

[15] By *Wrong-Sign combinations* we mean combinations of the same particles involved in the decay chain $D^{*+} \to D^0\tilde{\pi}^+$, $D^0 \to h^- l^+ \nu$, but with wrong charge correlation. The combinations $\tilde{\pi}^+(h^+ l^-)$ and $\tilde{\pi}^-(h^+ l^+)$ are both examples of WS combinations.

[16] For example, the decay $D^{*+} \to D^0\tilde{\pi}^+, D^0 \to K^-\pi^+\pi^0$, where the K^- is misidentified as a lepton l^-, will contaminate the WS $\pi^- l^+ \nu$ signal but not the RS.

[17] Monte Carlo studies suggest the remaining random background is largely due semileptonic decays which combine with random pions. For decays where the leptons are identified in the inner electromagnetic calorimeter and the inner muon system we estimate this background shape using non-D^* tagged $D^0 \to \pi^- e^+ \nu$ and $D^0 \to K^- e^+ \nu$ Monte Carlo decays. For decays in which the lepton is identified in the outer electromagnetic calorimeter the backgrounds are much higher and we obtain the random shape by combining the daughter hadron–lepton pair with soft pions from different data events.

[18] E653 Collab., K.Kodama et al., Phys. Lett B316, 455(1993).

(Note that in using the E653 result for $\frac{BR\ (D^+ \to \varrho^0 l^+ \nu)}{BR\ (D^+ \to K^{*0} l^+ \nu)}$, we symmetrize their statistical error and neglect their systematic error).

[19] CLEO Collab., A. Bean *et al.*, Phys. Lett. B317, 647 (1993).

[20] E687 Collab., P. L. Frabetti *et al.*, Phys. Lett. B307, 262 (1993).

[21] E691 Collab., J. C. Anjos *et al.*, Phys. Rev. D47, 1951 (1993).

[22] J.D. Richman and P.R. Burchat, *Leptonic and Semileptonic Decays of Charm and Bottom Hadrons*, UCSB-HEP-95-08, pag.75.

[23] If a single pole model parametrization for the form factor is assumed, the value of the pole mass is expected to be equal to the mass of the lowest vector meson resonance composed of the two quarks involved in the weak decay. Therefore the theoretically "expected" values are $M^K_{pole} = M(D^{*+}_s) = 2.11\ GeV/c^2$ for the $D^0 \to K^- l^+ \nu$ decay, and $M^{\pi}_{pole} = M(D^{*+}) = 2.01\ GeV/c^2$ for the $D^0 \to \pi^- l^+ \nu$ decay. The measured value for $D^0 \to K^- l^+ \nu$ is instead $M^K_{pole} = 1.90 \pm 0.09\ GeV/c^2$ (weighted average of references[19] and [24]). When studying the variation of M^{π}_{pole}, we therefore consider the range from $M^{\pi}_{pole} = 1.80\ GeV/c^2$ (a somewhat arbitrary value below $1.90\ GeV/c^2$) and $M^{\pi}_{pole} = 2.11\ GeV/c^2$.

[25] J. G. Korner and G. A. Schuler, Z. Phys. C38, 511 (1988).

[24] E687 Collab., P. L. Frabetti *et al.*, Phys. Lett. 364, 127 (1995).

[26] L.Jauneau, *"Spectra and Polarization in K_{μ_3}"*, in *Methods in Subnuclear Physics*, Edit by M.Nikolic, Vol.III (1969), p.123-186.

[27] Particle Data Group, L. Montanet *et al.*, Phys. Rev. D50, No. 3, (1994).

[28] We remind the reader that the only two mode specific independent yields which are returned by the fit are $Y_{K\ l\ \nu}$ and $Y_{\pi\ l\ \nu}$, all other yields are computed by assuming known branching ratios.

[29] Calculated assuming $|\frac{V_{cd}}{V_{cs}}|^2 = 0.051$

[30] To directly compare the relative branching ratios $\frac{B(D^+ \to \pi^0 l^+ \nu_l)}{B(D^+ \to \overline{K}^0 l^+ \nu_l)}$ and $\frac{B(D^0 \to \pi^- l^+ \nu_l)}{B(D^0 \to K^- l^+ \nu_l)}$ we multiplied the D^+ mode by a factor of two which arises from isospin considerations.

[31] V. Lubicz *et al.*, Phys. Lett. B274, 415 (1992).

[32] S. Narison, Phys. Lett. B377, 163 (1994).

[33] N. B. Demchuk *et al.*, INFN preprint INFN0ISS 95/18, Submitted to Sov. J. Nucl. Phys.

FIGURES

FIG. 1. Figures (a)-(c) are the $D^{*+} - D^0$ mass difference $D^0 \to K^- l^+ \nu$ data and fit histograms reconstructed with the muon sample, the electron sample, and the combined sample. The component labeled "BKG 1" is background from hadrons misidentified as leptons, and "BKG 2" is random combinatoric background. In Figures (d)-(f) we show the components of the fit associated with the $D^0 \to K^- l^+ \nu$ signals and the background from $D^0 \to K^{*-} l^+ \nu$ ("BKG 3").

FIG. 2. Figures (a)-(c) are the $D^{*+} - D^0$ mass difference $D^0 \to \pi^- l^+ \nu$ data and fit histograms reconstructed with the muon sample, the electron sample, and the combined sample. The component labeled "BKG 1" is background from hadrons misidentified as leptons, and "BKG 2" is random combinatoric background. In Figures (d)-(f) we show the components of the fit associated with the $D^0 \to \pi^- l^+ \nu$ signals, the background from $D^0 \to K^- l^+ \nu$, and the background from $D^0 \to K^{*-} l^+ \nu$ ("BKG 3").

FIG. 3. In Figure (a) we show our reconstruction of efficiency for a given pole mass divided by the reconstruction efficiency at the expected pole masses of $M^K_{pole} = 2.11\ GeV/c^2$ and $M^{\pi}_{pole} = 2.01\ GeV/c^2$. In Figure (b) we present the relative branching ratio measurement as a function of M^{π}_{pole} assuming $M^K_{pole} = 2.11\ GeV/c^2$. The value we choose to quote and our errors are shown as the solid and dashed lines respectively.

FIG. 4. In Figure (a) we show our measurement of the quantity $|\frac{V_{cd}}{V_{cs}}|^2\ |\frac{f^{\pi}_{+}(0)}{f^{K}_{+}(0)}|^2$ as a function of M^{π}_{pole} for the values $M^K_{pole} = 2.11\ GeV/c^2$ and $M^K_{pole} = 1.9\ GeV/c^2$. In

Figure (b) we present the quantity $|\frac{V_{cd}}{V_{cs}}|^2 \ |\frac{f_+^{\pi}(0)}{f_+^K(0)}|^2$ when using the linear approximation $f_+(q^2) = (1 + aq^2)$ for each of the two form factors. In both figure the solid line is the result we choose to quote and the dashed lines are the errors on that measurement.

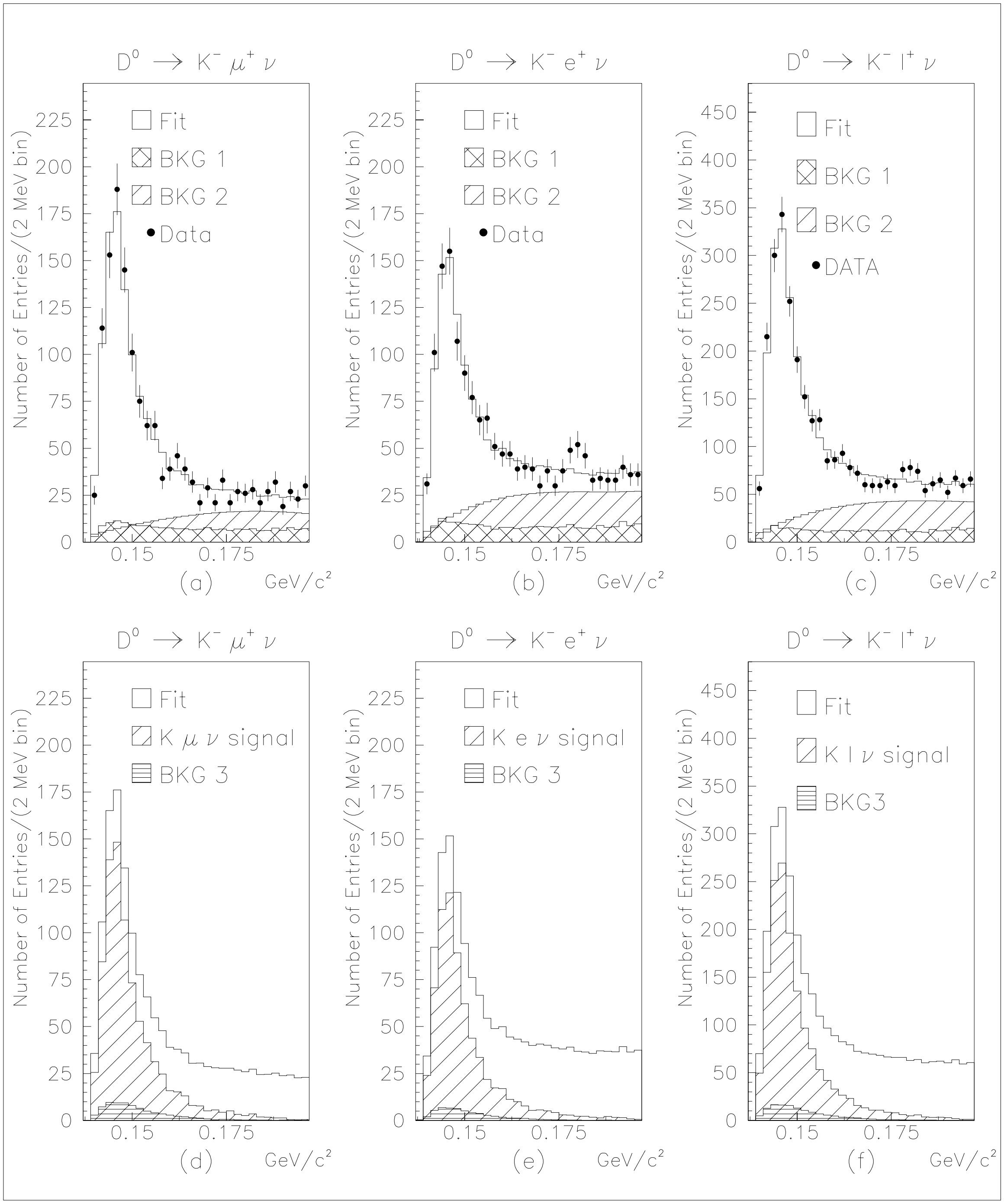

$D^0 \rightarrow K^- \mu^+ \nu$
$D^0 \rightarrow K^- e^+ \nu$
$D^0 \rightarrow K^- l^+ \nu$
Fit
BKG 1
BKG 2
Data
DATA
Number of Entries/(2 MeV bin)
GeV/c²
(a)
(b)
(c)
K μ ν signal
K e ν signal
K l ν signal
BKG 3
BKG3
(d)
(e)
(f)

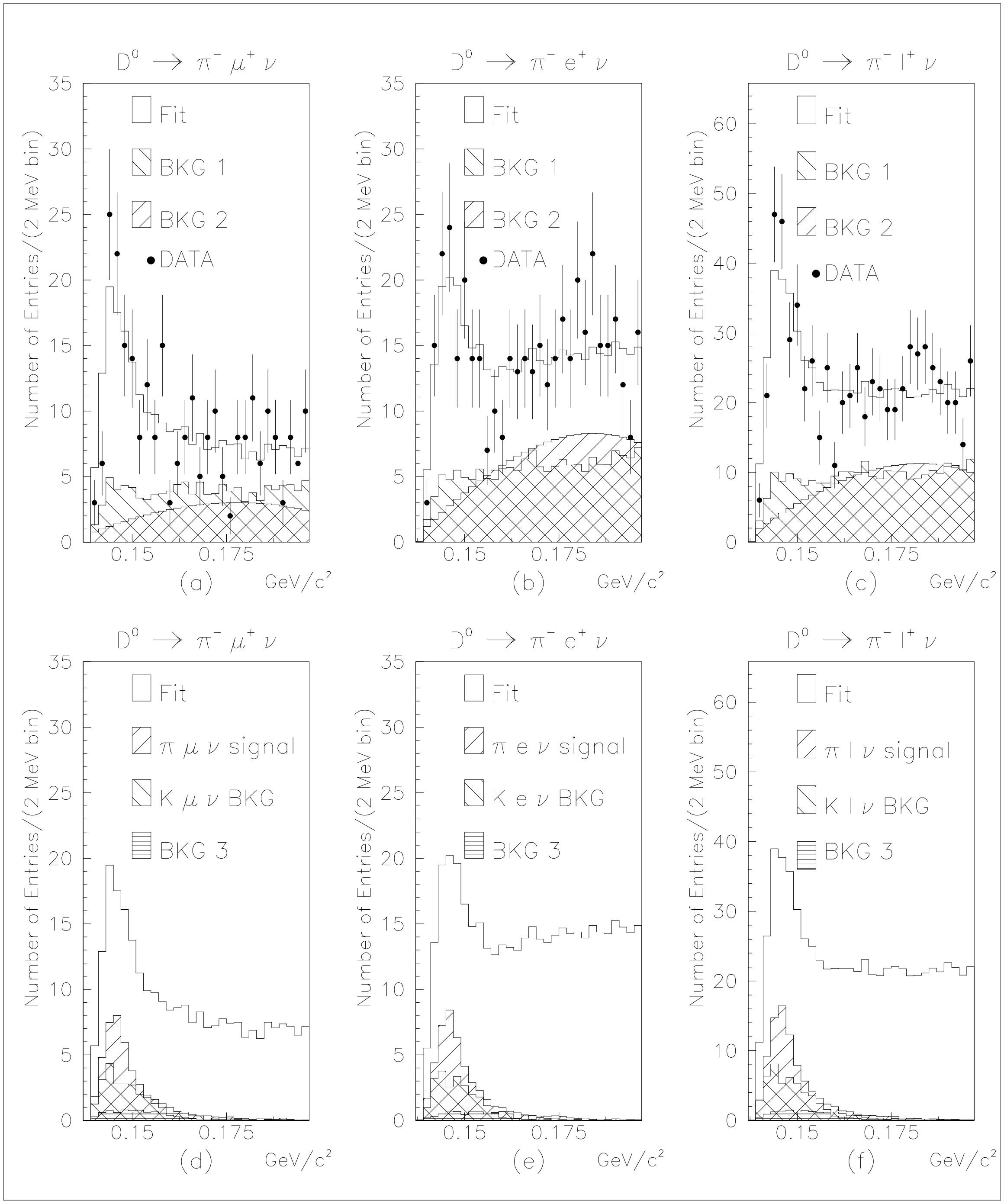

$D^0 \to \pi^- \mu^+ \nu$
$D^0 \to \pi^- e^+ \nu$
$D^0 \to \pi^- l^+ \nu$
Fit
BKG 1
BKG 2
DATA
$\pi\ \mu\ \nu$ signal
$K\ \mu\ \nu$ BKG
$\pi\ e\ \nu$ signal
$K\ e\ \nu$ BKG
$\pi\ l\ \nu$ signal
$K\ l\ \nu$ BKG
BKG 3
Number of Entries/(2 MeV bin)
GeV/c²
(a)
(b)
(c)
(d)
(e)
(f)

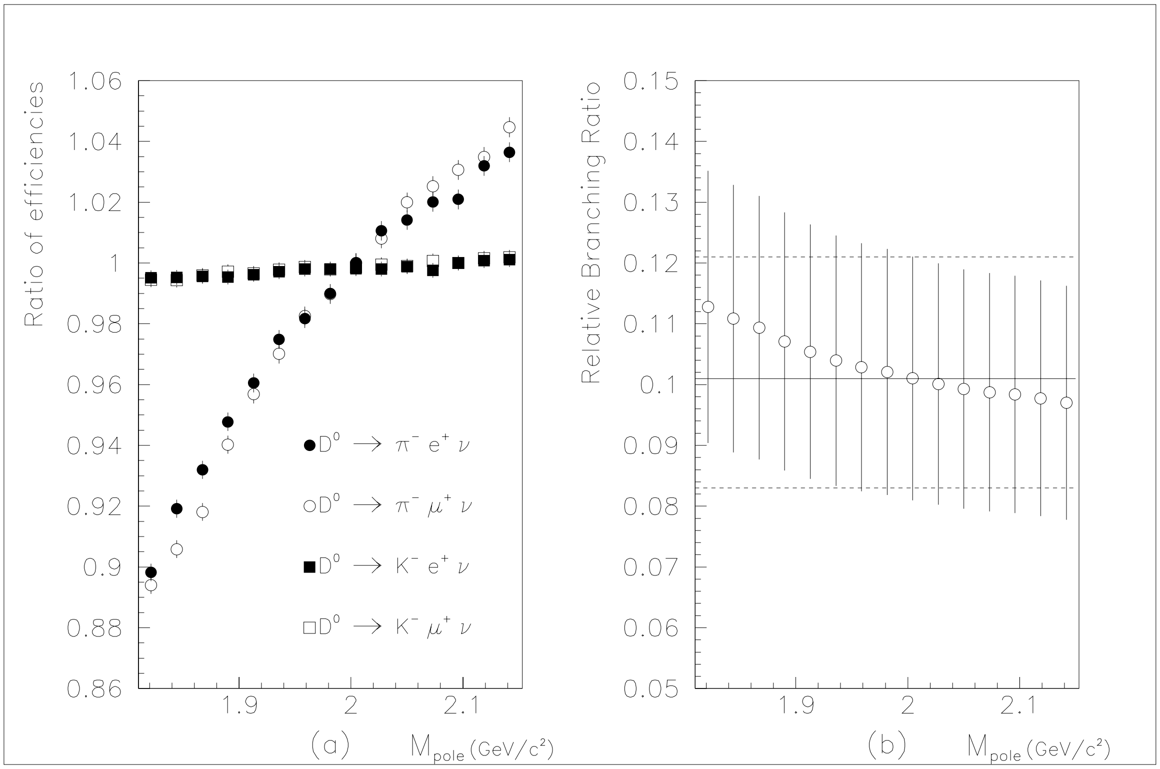

Ratio of efficiencies
1.06
1.04
1.02
1
0.98
0.96
0.94
0.92
0.9
0.88
0.86
$D^0 \rightarrow \pi^- e^+ \nu$
$D^0 \rightarrow \pi^- \mu^+ \nu$
$D^0 \rightarrow K^- e^+ \nu$
$D^0 \rightarrow K^- \mu^+ \nu$
1.9
2
2.1
(a)
M_{pole} (GeV/c^2)
Relative Branching Ratio
0.15
0.14
0.13
0.12
0.11
0.1
0.09
0.08
0.07
0.06
0.05
1.9
2
2.1
(b)
M_{pole} (GeV/c^2)

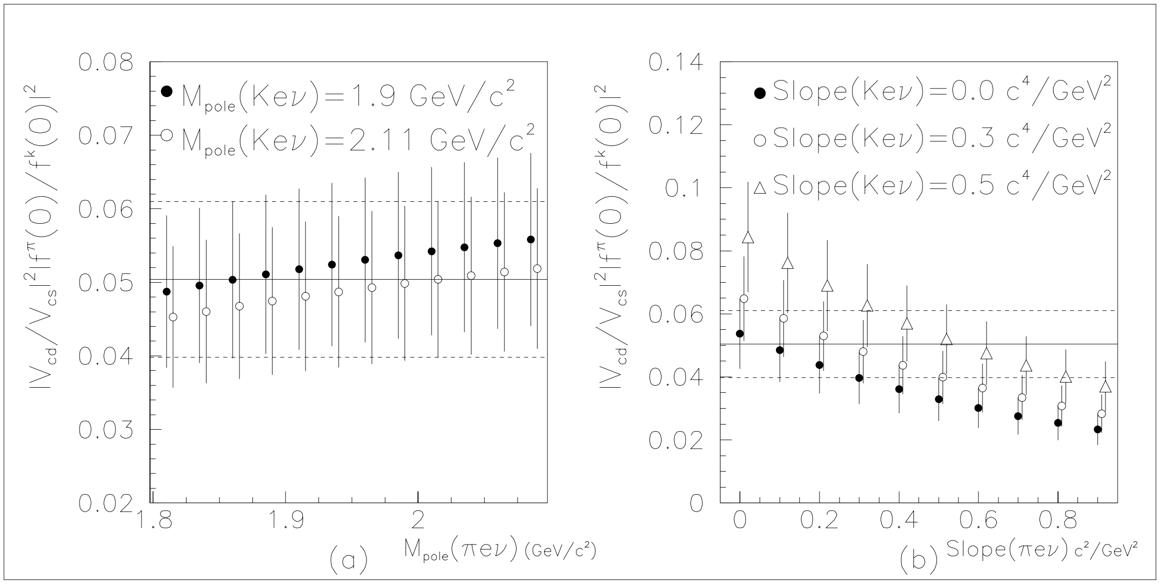

$M_{pole}(Ke\nu)=1.9\ GeV/c^2$
$M_{pole}(Ke\nu)=2.11\ GeV/c^2$
$|V_{cd}/V_{cs}|^2|f^\pi(0)/f^k(0)|^2$
$M_{pole}(\pi e\nu)$ (GeV/c^2)
(a)
$Slope(Ke\nu)=0.0\ c^4/GeV^2$
$Slope(Ke\nu)=0.3\ c^4/GeV^2$
$Slope(Ke\nu)=0.5\ c^4/GeV^2$
$|V_{cd}/V_{cs}|^2|f^\pi(0)/f^k(0)|^2$
(b)
$Slope(\pi e\nu)$ c^2/GeV^2